# Complex genetic architecture underlying the plasticity of tobacco leaf width provides insight into across-environment genomic prediction

**Li Liu[1#], Wei Liu[2#], Yiwen Sun[1], Yu Han[2], Ran Hao[3], Wenjia Zhang,[1] Linjie Guo[1], Jiarui Zhao[1], Yanjun Zan[1*], Lirui Cheng[1*], Huan Si[1*]**

[1]Tobacco Research Institute, Chinese Academy of Agricultural Sciences, Qingdao, CN-266000, China.
[2]Key Laboratory of Bio-resource an d Eco-environment of Ministry of Education, College of Life Sciences, Sichuan University, Chengdu, CN-610065, China.
[3]College of Forestry, Northwest Agriculture and Forestry University, Yangling, CN-712100, China.

[#]These authors contributed equally

[*]Corresponding authors

Huan Si

Email: sihuan@caas.cn

Lirui Cheng

Email: chenglirui@caas.cn

Yanjun Zan

Email: zanyanjun@caas.cn

**Abstract**

Phenotypic plasticity is the property of a given genotype to produce multiple phenotypes in response to changing environmental conditions. Understanding the genetic basis of phenotypic plasticity and establishing a predictive model is highly relevant for future agriculture under changing climate. Here, we investigated the genetic basis of leaf width plasticity in a tobacco MAGIC population across four different environments. Environmental changes not only resulted in differences in leaf width mean but also in leaf width plasticity. A total of 45 QTL were identified, including 14 QTL for leaf width mean and 43 for leaf width plasticity, with 12 overlap. Changes in the environment affected the magnitude of several QTL, thereby influencing phenotypic plasticity. We identified a QTL, qLW14, associated with leaf width plasticity and leaf width mean at Zhucheng, but had no significant impact at Guiyang, indicating that changes in the environment contributed to variations in leaf width plasticity. By integrating genetic diversity, environmental variation, and their interactions into a unified model, we were able to build a model for cross-environment predictions, and improved prediction accuracy by 7.2%. Overall, this study reveals complex genetic basis involving multiple alleles, and genotype interactions underlying variations of leaf width mean and plasticity. These findings contribute to assessing the role of plasticity in responding to climate or other environmental changes.

**Key words:** Tobacco, Leaf width, Phenotypic plasticity, QTL-by-environment interaction

## Introduction

Phenotypic plasticity refers to the phenomenon where individuals of the same genotype exhibit different phenotypes under different environmental conditions (Bradshaw, 1965; Pigliucci, 2005), or the ability of organisms to produce different phenotypes in response to varying environmental factors (Kliman, 2016; Nicotra et al., 2010). For organisms, phenotypic plasticity is a trait and possibly an important strategy to quickly adjust phenotypes according to environments, which potentially have effects on evolution (Bradshaw, 1965; Kusmec, de Leon, & Schnable, 2018; Sommer, 2020). With rapid climate changes, as sessile organisms, plants have evolved unique mechanisms to respond to environmental changes, including physiological, metabolic, growth, and developmental adjustments. Revealing the genetic basis of plasticity is crucial for enhancing our understanding of genetic variation of these complex traits in heterogeneous environments (Gillespie & Turelli, 1989; Ji et al., 2023; Jin et al., 2023; Kelly, 2019).

Tobacco (*Nicotiana tabacum* L.) is a model organism in plant genetics and synthetic biology. Tobacco leaf exhibits rich diversity and plasticity in morphology, and metabolic traits (Honarnejad & Shoai-Deylami, 2004; Legg & Collins, 1975; White, Pandeya, & Dirks, 1979), making it an ideal model organism for botanical and plant synthetic biology research. Therefore, genetic regulation of tobacco leaf morphological traits has attracted many attention during the past two decades. With the development of sequencing technology, the cost of sequencing has gradually decreased, the development of molecular markers has increased (Edwards et al., 2017; Khan et al., 2019; C. Wang et al., 2022), and genome-wide association analysis have been widely used in leaf morphological development, and many genes related to leaf number, width and length have been identified seat (Ahmed et al., 2019; Liu et al., 2022; Safdar et al., 2020; Zuo et al., 2022). Liu et al performed GWAS with a multiparent advanced generation inter-cross (MAGIC) population which consisting of 600 individuals and locating a tobacco plant height-related QTL at 140 cM on chromosome 13 (Liu et al.,

2022). However, little is known about the plasticity of leaf morphological development. While these studies provided insights on the genetic basis of leaf morphological traits, little investigation was performed on the genetic basis of leaf morphological traits plasticity.

In this study, we utilized a MAGIC population of 600 lines derived from eight parents to dissect the genetic basis of leaf width mean and leaf width plasticity across four environments. A total of 45 QTL associated with leaf width mean and plasticity were detected. We found that the dynamics change in QTL effects across environments was associated variation of leaf width plasticity, indicating that QTL-by-environment interactions may drive leaf width plasticity variation. Through integrating genetic diversity, environmental variation, and their interactions, we developed a model for site-specific predictions and improved accuracy considerably. Overall, this study reveals complex genetic basis involving multiple alleles, and genotype interactions underlying variations of leaf width mean and plasticity. These findings contribute to assessing the role of plasticity in responding to climate or other environmental changes.

## Results

### Tobacco leaf width mean variation within each of the four environments

We explored the genetic basis of leaf width mean and plasticity using 600 tobacco lines derived from a multi-parent advanced generation intercross （MAGIC）with genotypes using the 430K tobacco SNP array with 432,362 markers and leaf width (LW) measured under 4 different environments in Guiyang, Hunan (25°27′N 112°13′E), and Zhucheng, Shandong (35°59′N 119°24′E) in 2019 and 2020. In this study, the studied environment was abbreviated as: Hunan Guiyang in 2019 (GY19), Hunan Guiyang in 2020 (GY20), Shandong Zhucheng in 2019 (ZC19), Shandong Zhucheng in 2020 (ZC20). The leaf width mean and plasticity were abbreviated as LWm and LWp, respectively. LW displayed continuous variation, being the shortest at 13.5 cm and the longest at 37.5 cm. Changes in environment altered the mean and phenotypic variance of LWm (Vp; Fig

1B) across 4 environments. There was widespread reaction norm for LWm. For example, when the environment changed from ZC19 to GY19, the leaf width at Guiyang (LWm = 27.8cm) showed drastic difference in leaf width at Zhucheng (LWm = 21.8cm), leading to variation in LWp (Fig. 1B). This result indicates that environmental changes have an impact on both the LWm and LWp.

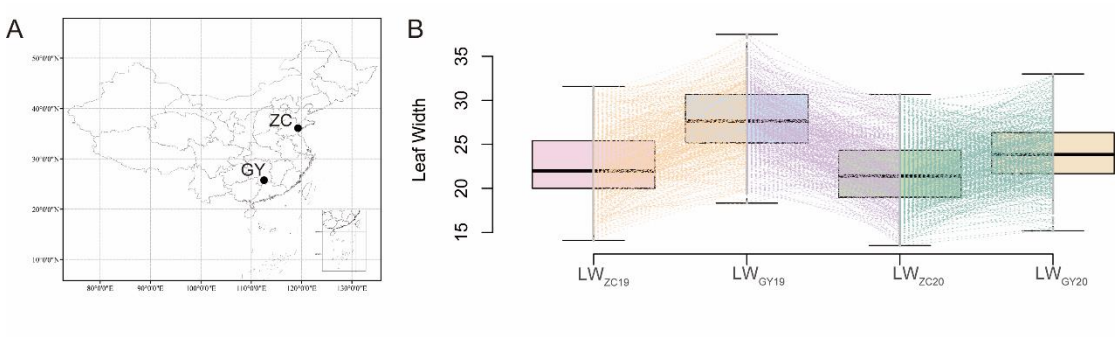


**Fig. 1A)** Geographical illustration of two Filed plantations, Zhucheng and Guiyang, where the MAGIC population was phenotyped. **B)** Boxplot of LWm measured at four environments.

**Environmental perturbation buffers/releases additive variation for LWm by altering the underlying genetic architecture**

There was a moderate variation (0.13-0.61; Fig 2A) in the estimated narrow-sense heritability ($h^2$) across different environmental conditions. Given that phenotypic variation ($V_p$) varied significantly among the four environments, the amount of additive genetic variation ($V_a$), estimated as $V_p$ times $h^2$, changed considerably from 4.1 to 11.2 (Fig 2B). These fluctuations in $V_a$ were likely caused by either altered genetic effects from one or multiple QTL or turning on/off of a completely new set of QTL, indicating the genetic architecture of LWm was dynamic across the four environments. This hypothesis was supported by the variation of pairwise genetic correlation from multivariate mixed model analysis (Fig 2C). The estimated genetic correlation between environments was as low as 0.4, suggesting considerable changes in the polygenic scores/breeding values across individuals. Collectively, these results illustrated that the genetic variance of LWm changed across these environments due to alterations in genetic architecture. In the following sections, we will quantify change and dissect the

genetic basis underlying LWm variation across environments.

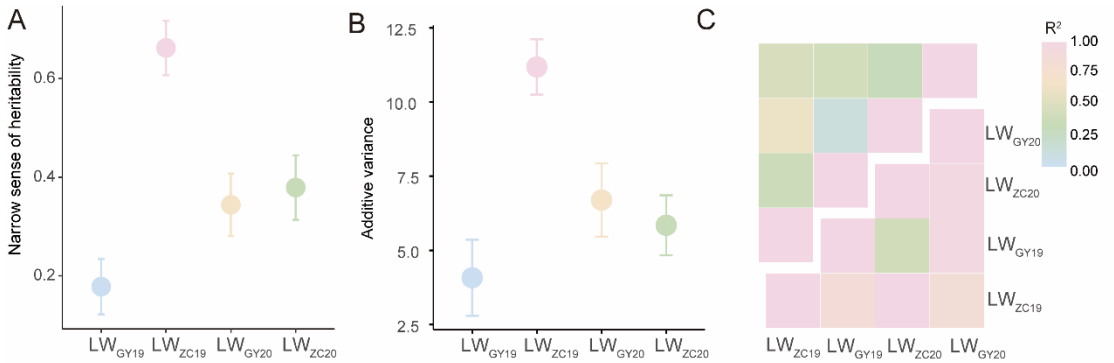


**Fig.2 A)** Estimated narrow-sense heritability ($h^2$) for LWm at each environment. Each dot represents a point estimate of $h^2$ indicated on the y-axis and the corresponding environment was labelled in the x-axis. Standard errors were plotted as error bars. **B)** Estimated additive variance at each environment. **C)** Upper triangular: Pairwise Spearman rank correlation among LWm measured under four environments. **C)** Lower triangular: Pairwise genetic correlation among LWm measured under four environments.

**Polygenic architecture underlying tobacco LWm variation and LWp variation**

There was a widespread reaction norm for LWm. At population level, the median of LWm in Zhucheng is significantly smaller than that in Guiyang (Fig. 1B), resulting in variation in LWp. We, therefore, quantified LWp using two types of metrics. The first type involved two measures including Finlay–Wilkinson Regression (FWR), and across environment variance in rank transformed LWm (VarR) quantifying the overall plasticity (OP) of LW across all environments. The second metric involved assessing pairwise LWm differences for all possible pairs of environments, quantifying specific changes across paired environments and resulting in a total of 6 specific plasticity (SP) measures. Almost all the plasticity measurements were continually distributed with intermediate to high narrow sense heritability (0.02-0.61).

A total of 45 QTL were identified for LWm and LWp using genome-wide association analysis (GWA) (Fig. 3A), including 14 QTL for LWm, 9 QTL for leaf width BLUP and 43 QTL for LWp with variable degrees of overlaps, indicating a shared genetic

basis between LWm, LWp and BLUP (Fig. 3C).

By contrasting genetic effects of QTL across sites, two types of QTL, whose effects changed in magnitude, were associated with LWp For example, qLW1-3 showed a significant effect for $LW_{ZC19}$ (3.6 ± 0.3cm; P = 4.8 x $10^{-16}$; Fig. 3D), $LW_{ZC20}$ (2.7 ± 0.4cm; P = 4.4 x $10^{-9}$) as well as on the specific plasticity measures $LW_{GY19\text{-}ZC20}$ (P = 5.9 x $10^{-8}$; Fig. 3D) and $LW_{ZC19\text{-}GY19}$ (P = 2.2 x $10^{-14}$; Fig. 3D), indicating changes in the magnitude of genetic effects contributed to the variation of LW plasticity. In contrast, qLW9-1 (Fig. 3E), was exclusively detected for several LWp but not for any of the LWm and $LW_{BLUP}$ measurements. Altogether, these results suggested that changes in magnitude of genetic effects across sites caused variation in plasticity. The changing genetic effects highlighted the role of QTL by environment interaction in the variation of LWm and LWp.

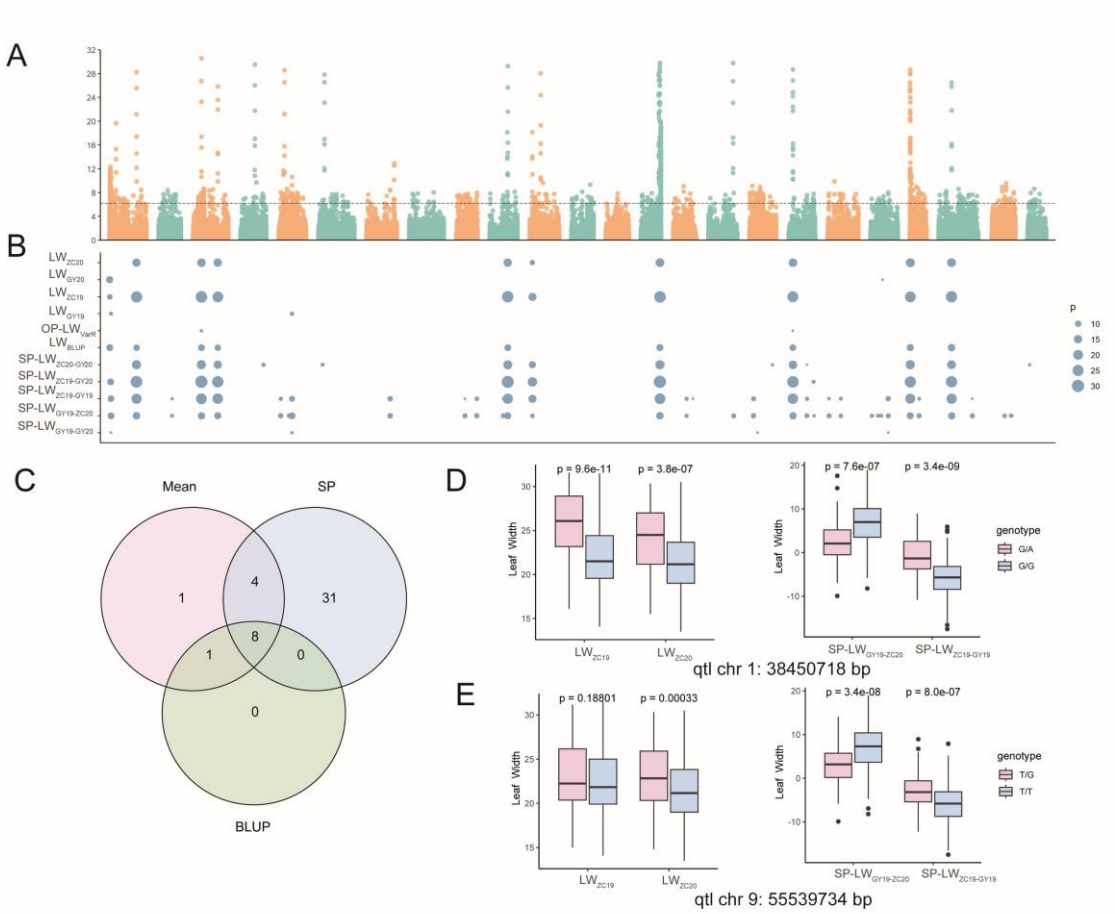


**Fig. 3 A)** Manhattan plots overlaying genome-wide association analysis results for the mean, plasticity measurements and BLUP for LW. The black horizontal dashed line

indicated the Bonferroni-corrected genome-wide significance threshold derived as 0.05/Me (Me is the effective number of independent markers; Methods) **B)** QTL associated with the LWm and LWp measured at four environments and the $LW_{BLUP}$ (y-axis). Each dot represents a SNP, and the size of the dot is proportional to its -Log10 p value, as indicated in the legend on the right. Loci with a p value above the genome-wide significance threshold are colored in blue. **C)** Venn diagram illustrating the overlap of QTL detected for the 3 types of LW measurements. **D) and E)** Genotype-to-phenotype maps for LWm and $LW_{SP}$ at Chr 1: 38450718bp, Chr 9: 55539734bp.

**qLW14 associated with LWm and LWp measurements**

We detected a QTL，qLW14 located at chromosome 14: 116-123 Mb, associated with LWm at Zhucheng ($LW_{ZC19}$, $LW_{ZC20}$) and multiple LWp measurements (SP-$LW_{GY19-ZC20}$, SP-$LW_{ZC19-GY19}$, SP-$LW_{ZC19-GY20}$, SP-$LW_{ZC20-GY20}$, Fig. 4A). Among the eight parental lines, haplotype analysis revealed two main haplotypes, with one parent *Vam* harbouring a deletion of approximately 3Mb at the qLW14 (121-124 Mb), while no deletions were observed in the remaining seven parents (Fig. 4B). Linkage disequilibrium analysis revealed a high level of linkage disequilibrium at this region, which overlapped with the deleted fragment in *Vam* (Fig. 4C). Phenotypic analysis showed that lines carrying this deletion exhibited a 20% increase in leaf width at Zhucheng in comparison to that for lines without the deletion (Fig. 4D). In contrast, lines carrying this deletion did not significantly increase leaf width at Guiyang. Overall these results highlighted a general contribution from qLW14 by environment interaction to variation of LWp (Fig. 4E).

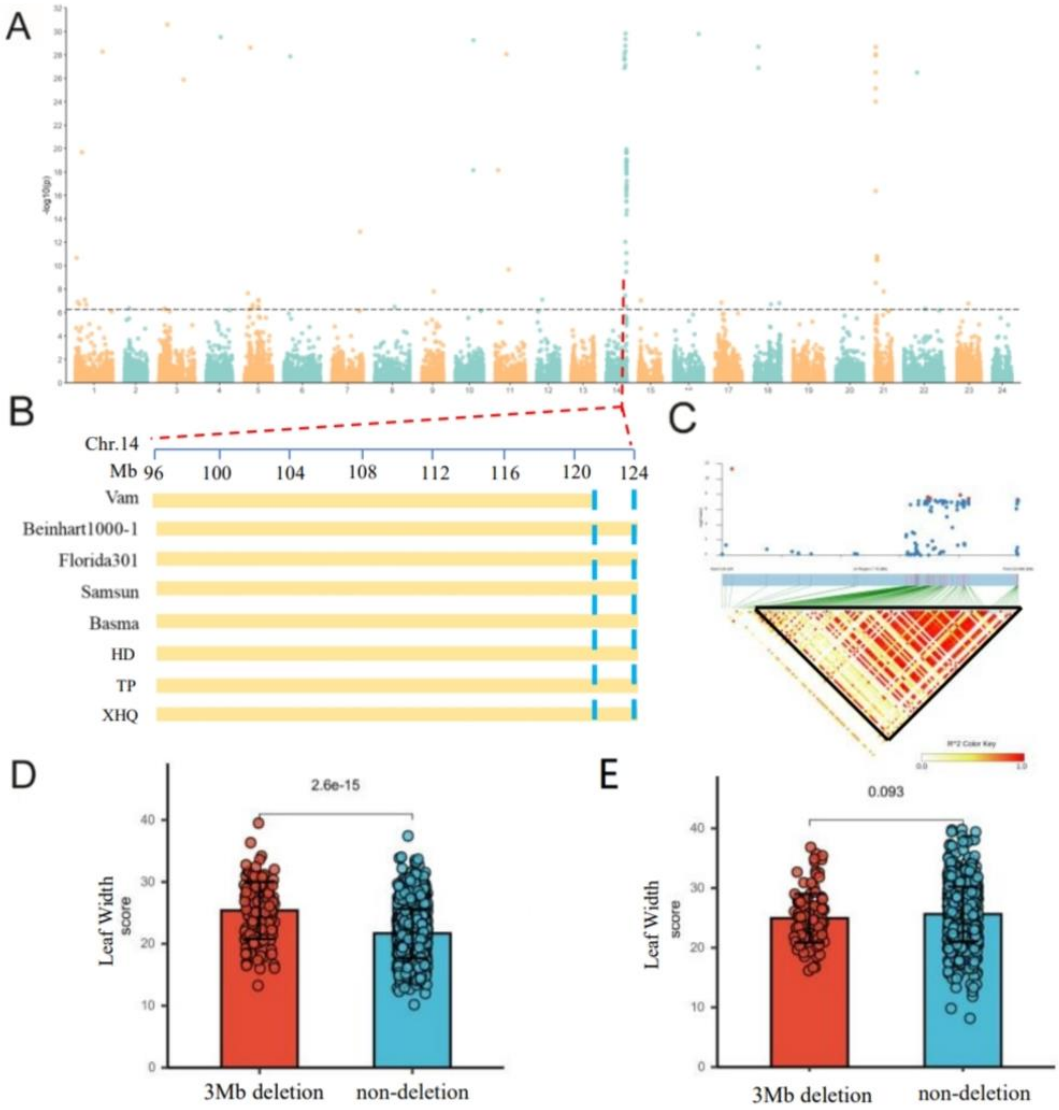


**Fig. 4A)** Manhattan plot for plasticity measurement $LW_{ZC19\text{-}GY20}$. The black horizontal dashed line represents the Bonferroni-corrected genome-wide significance threshold of 0.05/Me (Me is the effective number of independent markers; Methods). **B)** Haplotype analysis from re-sequenced eight parents for MAGIC population (*Vam*, *Beinhart1000-1*, *Florida301*, *Samsun*, *Basma*, HD: *honghuadajianyuan*, TP: *tangpeng*, XHQ: *xiaohuaqing*) revealed a 3Mb deletion in *Vam*. **C)** LD heatmap showing the region surrounding a strong peak (chromosome 14: 116 Mb–124 Mb). Difference in leaf width of the two haplotype lines qLW14 in the year of 2019 and 2020 at Zhucheng, Shandong **D)** and Guiyang, Hunan **E).**

**Accounting for dynamics in genetic architecture improved LWm prediction across environment**

Here, we evaluated the potential of integrating genetic diversity, environmental variation, and their interaction in complex trait prediction by jointly modelling

genotype, environment, and their interaction (referred to as GEAI model, Methods). Two cross-validation schemes were considered. First, we explored the ability to predict untested lines (Newly developed lines) at the four environments using five-fold cross-validation. In this scenario, 80% of the lines with phenotype measured from all the four environments were randomly selected as training set and the remaining 20% lines, whose phenotypes were masked as NA, were used as test set (Fig. 5A, 5B). Within site Pearson correlation (r) between predicted and measured phenotype were used to evaluate the accuracy of predicted phenotype at each of the four environments. Compared with the GBLUP, with a universal prediction for all sites, our model not only provided site-specific predictions but also increased prediction accuracy. The averaged prediction accuracy for LW increased by 8.7%.

In the second scenario, we performed prediction for novel sites without any tested lines by utilizing phenotypic data from three out of the four environments as the training set, while the phenotype data from the remaining environment served as the test set. Compared to the GBLUP model, our GEAI model exhibited an average improvement of 7.2% in prediction accuracy. This substantial enhancement underscores the effectiveness of our GEAI model in capturing and leveraging genotype-environment interactions to enhance prediction accuracy across different environmental contexts. Overall, our study highlighted the potential of intergrading QTL by environment interaction in understanding complex traits variation and predictions.

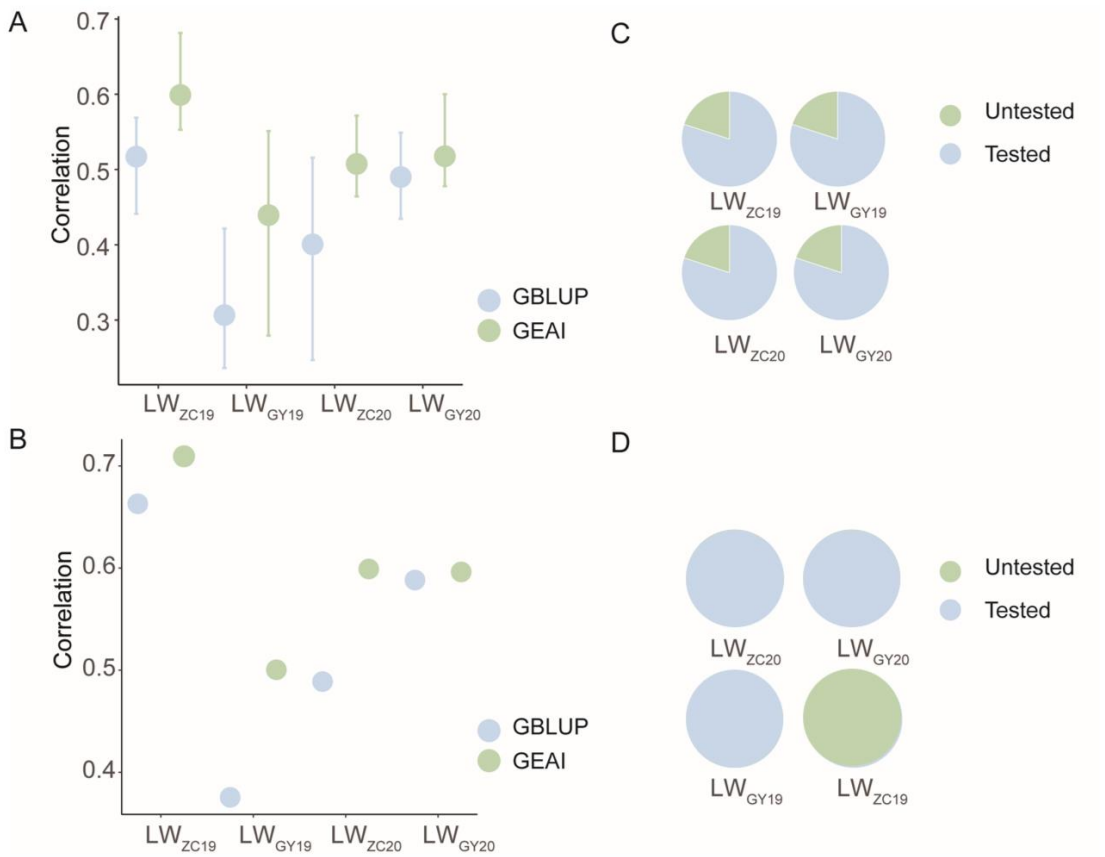


**Fig 5 A)** Use 5-fold cross-validation to predict the phenotypes of the remaining 20% lines in each environment. **B)** Use the phenotypes of all strains in three environments in the four environments as training set for LW, and the remaining environments as a test set. **C)** Schematic illustration of the prediction design for **A)**. **D)** Schematic illustration of the prediction design for **B)**, with $LW_{ZC20}$, $LW_{GY20}$, and $LW_{GY19}$ as training set and $LW_{ZC19}$ as the tested set.

## Discussion

Consistent with studies in maize and rice (Guo et al., 2020; Ji et al., 2023), we found a considerable proportion of QTL (33%) associated with LWp were shared with those associated with LWm, suggesting a shared genetic basis between LWm and LWp. However, due to a lack of environmental factor data, we were not able to definitively determine which environmental factors influence the plasticity of leaf width. Further investigation is needed to explore the specific roles of environmental factors in the variation of LWm and LWp.

Haplotype analysis on qLW14 revealed the presence of multiple duplicate MADS-box transcription factors. The candidate gene MADS-box has been confirmed to be involved in leaf development in *Arabidopsis* and *tomato*. In *Arabidopsis*, a MADS-box member *FRUITFULL(FUL)* affects leaf development by affecting vascular bundle development (Bemer et al., 2017); in *tomato*, a MADS-box member *SlMBP21* affects leaf development by inhibiting genes involved in determining seed development (Y.-s. WANG et al., 2021). Although the candidate interval of qLW14 is still large in our results, with the advancement of multi-gene editing technologies such as CRISPR/LbCpf1, it is worthwhile to conduct fine mapping and functional verification of potential candidate genes for this QTL.

We constructed a genomic prediction model that considers genotype-environment interactions. When using three of the environments as training set to predict phenotypes in the remaining environment, this model outperformed Genomic Best Linear Unbiased Prediction (GBLUP). This superiority of the GEAI model is attributed to its inclusion of interactions between detectable QTL and environmental conditions. Due to a lack of various environmental factor data, we cannot confirm the interactions between QTL and specific environmental factors, which requires further exploration. Despite its imperfections, we recommend using the GEAI model for cross-environment trait prediction, as it can further enhance prediction accuracy. By establishing a prediction model that responds to environmental changes, we can predict leaf width phenotypes under different environments, laying the foundation for improving the accuracy of genome-wide prediction of agronomic traits under multiple environments.

## Methods

### *Phenotype and Genotype*

A total of eight different tobacco varieties were utilized as parents to develop the MAGIC population. These included *Beinhart1000-1* and *Florida301*, which is cigar

tobacco varieties; *Basma* and *Samsun*, belonging to oriental tobacco; *Xiaohuaqing* (XHQ) and *Tangpeng* (TP) from sun-cured tobacco; *Vam*, a variety of Virginia tobacco; and finally, the flue-cured tobacco variety *Honghuadajinyuan* (HD). Initially, these eight parents were crossed in pairs, resulting in four two-way crosses. Subsequently, the offspring from these crosses were subjected to incomplete diallel crossing to generate four-way crosses. Further crossing led to the production of eight-way crosses. These eight-way crosses were then subjected to random mating, yielding a total of 320 eight-way crossbreds. From these 320 eight-way crossbreds, three individual plants were selected per crossbred, and then propagated for five generations through the single seed descent (SSD) method, resulting in the establishment of over 800 eight-way tobacco MAGIC inbred lines.

In 2019 and 2020, the MAGIC population, along with the eight parents, were planted separately in Shandong Zhucheng, China, and Guiyang, Hunan, China, respectively. Randomized complete block design was employed with two replicates. Replicate of each line comprised two rows of 10-plants each, with row length of 10 m, row spacing of 1.2 m, and plant spacing of 0.5 m.

During each experiment, five randomly selected plants were selected for phenotypic evaluation, and the average value was analyzed. Leaf width was defined by measuring the width of the blade perpendicular to the main vein for the middle leaf .

Genotyping was conducted using a tobacco SNP chip with 432,362 markers from the Zhengzhou Tobacco Research Institute of the China Tobacco Corporation. Detailed information regarding genotyping and SNP calling procedures can be found in a previous study (Yuan et al., 2022).

***Calculation of kinship heritability and genetic correlation***

Kinship heritability was estimated using a mixed linear model:

$$\overline{y} = \mu + Zb + e \quad (1)$$

Here, $\overline{y}$ is LWm of 600 lines. $\mu$ is the intercept representing the population mean. $Z$ is the corresponding design matrix that satisfies $ZZ^T = G$, where $G$ is the genomic kinship matrix estimated from GCTA (Yang, Lee, Goddard, & Visscher, 2011). Therefore, $b$ follows a normal distribution $N(0, I\sigma_g^2)$. $e$ is the residual with $e \sim N(0, I\sigma_e^2)$. Kinship heritability is calculated as interclass correlation $h^2 = \frac{\sigma_g^2}{\sigma_g^2 + \sigma_e^2}$. All the analysis were performed in GCTA. Pairwise genetic correlation among LWm measured under the four environments was estimated by a multivariant mixed linear model in ASReml.

***Quantification of plasticity measurements***

Since all the MAGIC lines were phenotyped for LW across four environments, we quantified and studied the genetics of LW plasticity in response to environmental variation. Here, the phenotypic plasticity was classified into two categorie. The first category is overall plasticity describing plasticity across all the studied environments, while the second category-specific plasticity is more unique to certain pairs of sites, which only captures the plasticity across two environments. The motivation underlying such classification is that some individuals are more robust across most of the studied sites except only one or a few sites, while other individuals are plastic among most of the sites. One metric, pairwise difference in phenotypic value between two sites, was used to quantify the specific plasticity. In addition, two additional approaches were used to quantify the overall plasticity. First the across environment variance (VarR) (Vanous et al., 2019) of the rank transformed phenotype proposed in Vanous et al., 2019 was used, was also used to account for the mean difference. The fourth score for the overall plasticity (FWR) (Finlay & Wilkinson, 1963; Lian & de Los Campos, 2016) applies Finlay-Wilkinson Regression to partition the phenotype into two components, one is constant across environments and another responds dynamically to environmental changes. Using the linear mixed model, the phenotype of each line is partitioned into these two components and the plasticity component is used as a measurement of

plasticity. In total, the described approaches resulted in eight measurements of phenotypic plasticity (abbreviated as SP, VarR and FWR).

***Genome-wide association analysis for LW mean/BLUP and plasticity measurements***

Genome-wide association analysis was conducted using a linear mixed model as implemented in GCTA. We applied a significance threshold of $p < 0.05/Me$ for SNPs, where Me represents the number of independent SNPs estimated following methods described by Li et al. (Li, Yeung, Cherny, & Sham, 2012). The effect sizes of identified quantitative trait loci (QTL) were obtained from the GCTA output. The effect sizes for each SNP were estimated using the aforementioned mixed linear model.

***Predicting the site-specific performance of the LW***

We fitted the following model to predict the performance of each site for LW.

$$\mathrm{Y} = X_1\beta_1 + \mathrm{Zu} + \mathrm{e} \quad (2)$$

$$\mathrm{Y} = X_2\beta_2 + \mathrm{Zu} + \mathrm{e} \quad (3)$$

Here, Y is a vector of length n*p (n = 600, the number of individuals; p = 4, the number of sites; n*p = 2400), representing the trait means measured at four sites. u is a vector of length n*p, representing the breeding value of the n maize line, and e is the randomly distributed residual with length n*p. The Z matrix satisfies $ZZ'=G \otimes I$, where G is the identity by state (IBS) matrix and I is a diagonal matrix of pxp. $X_1$ is a design matrix with one column of 1 representing column mean and additional 3 columns representing the environmental effects from the remaining 3 sites, and $\beta_1$ is a vector of corresponding effect sizes. $X_2$ includes all the columns from $X_1$ and additional columns with genotypes of the k QTL associated with the mean and plasticity measures of the tested trait, and additional columns representing the interaction between the k QTL and the five sites, capturing the effects from QTL by environment factor interaction. The fitted values from model 3 were referred to as GBLUP predictions

while the fitted values from model 4 were referred to as GEAI predictions. These models were fitted using rrBLUP (Endelman, 2011) package in R (https://www.R-project.org/). In the first case, 80% of the lines with phenotype measured from all the five sites were used as training set and the remaining 20% lines, whose phenotypes were masked as NA, were used as test set. Within site $r^2$ between predicted and measured phenotype were used to evaluate the accuracy of predicted phenotype at each of the four sites. In the second case, we randomly selected all lines with measured phenotypes from three sites to be used as the training set, and the remaining one site was used as the test set and masked to NA. Accuracy was estimated as the regression r2 between the measured and predicted phenotype within each locus. All the lines with measured phenotype were used as training set and lines masked as NA was used as test set. Accuracies were estimated as the regression $r^2$ between measured and predicted phenotypes within each site.

**Funding**

This research was funded by the State key Key Research & Development Project-Youth Scientist Program (2023YFD1202400), National Science Foundation of China (32200503), China National Tobacco Corporation (110202101040 JY-17, Taishan Young Scholar Program and Distinguished Overseas Young Talents Program from Shandong province, Agricultural Science and Technology Innovation Program (ASTIP-TRIC01) from Chinese Academy Agriculture Sciences.

**Author Contributions**

Conceptualization, L.L., W.L., Y.H., R.H.; methodology, Y.H., R.H., Y.Z., H.S.; formal analysis, L.L., W.L.; Y.H.; investigation, Y.S., W.Z., L.C.; data collection and curation, L.C., Y.Z., H.S., W.Z., Y.S., L.G.; writing original draft preparation, L.L., W.L.; writing reviewing and editing, L.L., W.L., Y.Z., H.S.; visualization, L.L., W.L, Y.H; supervision, Y.Z., H.S.; funding acquisition, Y.Z., H.S., L.C. All authors have read and agreed to the published current version of the manuscript.

**The authors have no conflicts of interest to declare.**

## Reference


Ahmed, W., Xia, Y., Zhang, H., Li, R., Bai, G., Siddique, K. H., & Guo, P. (2019). Identification of conserved and novel miRNAs responsive to heat stress in flowering Chinese cabbage using high-throughput sequencing. *Scientific Reports, 9*(1), 14922.

Bemer, M., van Mourik, H., Muiño, J. M., Ferrándiz, C., Kaufmann, K., & Angenent, G. C. (2017). FRUITFULL controls SAUR10 expression and regulates Arabidopsis growth and architecture. *Journal of experimental botany, 68*(13), 3391-3403.

Bradshaw, A. D. (1965). Evolutionary significance of phenotypic plasticity in plants. *Advances in genetics, 13*, 115-155.

Edwards, K. D., Fernandez-Pozo, N., Drake-Stowe, K., Humphry, M., Evans, A. D., Bombarely, A., . . . Kernodle, S. P. (2017). A reference genome for Nicotiana tabacum enables map-based cloning of homeologous loci implicated in nitrogen utilization efficiency. *BMC genomics, 18*, 1-14.

Endelman, J. (2011). Ridge regression and other kernels for genomic selection with R package rrBLUP. Plant Genome 4: 250–255. In.

Finlay, K., & Wilkinson, G. (1963). The analysis of adaptation in a plant-breeding programme. *Australian journal of agricultural research, 14*(6), 742-754.

Gillespie, J. H., & Turelli, M. (1989). Genotype-environment interactions and the maintenance of polygenic variation. *Genetics, 121*(1), 129-138.

Guo, T., Mu, Q., Wang, J., Vanous, A. E., Onogi, A., Iwata, H., . . . Yu, J. (2020). Dynamic effects of interacting genes underlying rice flowering-time phenotypic plasticity and global adaptation. *Genome Research, 30*(5), 673-683.

Honarnejad, R., & Shoai-Deylami, M. (2004). Gene effects, combining ability and correlation of characteristics in F2 populations of burley tobacco cultivars (Nicotiana tabacum L.). *JWSS-Isfahan University of Technology, 8*(2), 135-148.

Ji, Y., Han, Y., Dai, Y., Hao, F., Feng, X., Chen, Q., . . . Zhang, W. (2023). Polygenic basis of strong and rapid flowering time response to environment perturbations in wild Arabidopsis thaliana population. *bioRxiv*, 2023.2007. 2002.547444.

Jin, M., Liu, H., Liu, X., Guo, T., Guo, J., Yin, Y., . . . Wang, X. (2023). Complex genetic architecture underlying the plasticity of maize agronomic traits. *Plant Communications, 4*(3).

Kelly, M. (2019). Adaptation to climate change through genetic accommodation and assimilation of plastic phenotypes. *Philosophical Transactions of the Royal Society B, 374*(1768), 20180176.

Khan, S. U., Yangmiao, J., Liu, S., Zhang, K., Khan, M. H. U., Zhai, Y., . . . Zhou, Y. (2019). Genome-wide association studies in the genetic dissection of ovule number, seed number, and seed weight in Brassica napus L. *Industrial Crops and Products, 142*, 111877.

Kliman, R. M. (2016). *Encyclopedia of evolutionary biology*: Academic Press.

Kusmec, A., de Leon, N., & Schnable, P. S. (2018). Harnessing phenotypic plasticity to improve maize yields. *Frontiers in Plant Science, 9*, 410186.

Legg, P. D., & Collins, G. (1975). Genetic parameters in a Ky 14 x Ky Ex 42 burley population of

Nicotiana tabacum L. *Theoretical and Applied Genetics, 45*(6), 264-267.

Li, M.-X., Yeung, J. M., Cherny, S. S., & Sham, P. C. (2012). Evaluating the effective numbers of independent tests and significant p-value thresholds in commercial genotyping arrays and public imputation reference datasets. *Human genetics, 131*, 747-756.

Lian, L., & de Los Campos, G. (2016). FW: an R package for Finlay–Wilkinson regression that incorporates genomic/pedigree information and covariance structures between environments. *G3: Genes, Genomes, Genetics, 6*(3), 589-597.

Liu, Y., Yuan, G., Si, H., Sun, Y., Jiang, Z., Liu, D., . . . Luo, Z. (2022). Identification of QTLs associated with agronomic traits in tobacco via a biparental population and an eight-way MAGIC population. *Frontiers in Plant Science, 13*, 878267.

Nicotra, A. B., Atkin, O. K., Bonser, S. P., Davidson, A. M., Finnegan, E. J., Mathesius, U., . . . Valladares, F. (2010). Plant phenotypic plasticity in a changing climate. *Trends in plant science, 15*(12), 684-692.

Pigliucci, M. (2005). Evolution of phenotypic plasticity: where are we going now? *Trends in ecology & evolution, 20*(9), 481-486.

Safdar, L. B., Almas, F., Sarfraz, S., Ejaz, M., Ali, Z., Mahmood, Z., . . . Liu, S. (2020). Genome-wide association study identifies five new cadmium uptake loci in wheat. *The Plant Genome, 13*(2), e20030.

Sommer, R. J. (2020). Phenotypic plasticity: from theory and genetics to current and future challenges. *Genetics, 215*(1), 1-13.

Vanous, A., Gardner, C., Blanco, M., Martin-Schwarze, A., Wang, J., Li, X., . . . Edwards, J. (2019). Stability analysis of kernel quality traits in exotic-derived doubled haploid maize lines. *The Plant Genome, 12*(1), 170114.

Wang, C., Ma, Q., Xie, X., Zhang, X., Yang, D., Su, J., . . . Lin, H. (2022). Identification of favorable haplotypes/alleles and candidate genes for three plant architecture-related traits via a restricted two-stage multilocus genome-wide association study in upland cotton. *Industrial Crops and Products, 177*, 114458.

WANG, Y.-s., GUO, P.-y., ZHANG, J.-l., XIE, Q.-l., Hui, S., HU, Z.-l., & CHEN, G.-p. (2021). Overexpression of the MADS-box gene SlMBP21 alters leaf morphology and affects reproductive development in tomato. *Journal of Integrative Agriculture, 20*(12), 3170-3185.

White, F., Pandeya, R., & Dirks, V. (1979). Correlation studies among and between agronomic, chemical, physical and smoke characteristics in flue-cured tobacco (Nicotiana tabacum L.). *Canadian Journal of Plant Science, 59*(1), 111-120.

Yang, J., Lee, S. H., Goddard, M. E., & Visscher, P. M. (2011). GCTA: a tool for genome-wide complex trait analysis. *The American Journal of Human Genetics, 88*(1), 76-82.

Yuan, G., Sun, K., Yu, W., Jiang, Z., Jiang, C., Liu, D., . . . Wang, Y. (2022). Development of a MAGIC population and high-resolution quantitative trait mapping for nicotine content in tobacco. *Front Plant Sci, 13*, 1086950. doi:10.3389/fpls.2022.1086950

Zuo, J.-F., Ikram, M., Liu, J.-Y., Han, C.-Y., Niu, Y., Dunwell, J. M., & Zhang, Y.-M. (2022). Domestication and improvement genes reveal the differences of seed size-and oil-related traits in soybean domestication and improvement. *Computational and Structural Biotechnology Journal, 20*, 2951-2964.